Available online at www.sciencedirect.com
SCIENCE DIRECT®
European Journal of Mechanics B/Fluids 23 (2004) 415–425

Turbulent dissipation near absolute zero

Carlo F. Barenghi

School of Mathematics, University of Newcastle, Newcastle-upon-Tyne NE1 7RU, UK

Received 30 January 2003; received in revised form 20 June 2003; accepted 30 October 2003

Abstract

The superfluid component of liquid helium has exactly zero viscosity and its rotational motion is constrained by quantum mechanics to very thin vortex filaments of the same circulation. When liquid helium is made turbulent the vortex filaments form a disordered tangle. This article critically reviews recent experiments and calculations to explain the surprising observation that near absolute zero, in the absence of viscous effects, turbulent kinetic energy decays, and to highlight similarities and differences between superfluid turbulence and ordinary classical turbulence.

Keywords: Turbulence; Superfluid; Vortex line; Helium; Energy spectrum; Vortex reconnection

1. Introduction

Helium is a gas at room temperature and pressure. To turn gaseous helium into liquid helium the temperature must be reduced to almost absolute zero (the boiling point is only $T = 4.21$ K). Liquid helium exists in two phases: a high temperature phase (called helium I) and a low temperature phase (called helium II). Helium I and helium II are separated by a phase transition (called the lambda transition) which takes place at the lambda temperature $T_\lambda = 2.17$ K at saturated vapour pressure. Helium II is of great interest to physicists (its remarkable properties are a consequence of quantum mechanics) as well as to engineers (it is used as cryogenic coolant).

This article is concerned not with the fundamental physics nor with the applications. My aim is to discuss the fluid dynamics properties of helium II, particularly its turbulence state. I shall review recent results and put together a picture which explains the experimental observations, at least in a qualitative way. In doing so I shall also highlight the similarities and the differences between turbulent helium II (quantum turbulence) and ordinary (classical) turbulence. Finally, I shall point to the further studies which are needed to achieve more quantitative understanding of turbulence near absolute zero.

2. The two-fluid theory

According to Landau's two-fluid theory, helium II is the intimate mixture of two fluid components, the normal fluid and the superfluid [1]. The first component consists of thermally excited states which form a viscous fluid which carries the entire entropy content of the liquid; its density is ρ_n and its velocity is $\mathbf{v}_n$. The second component is related to the quantum ground state and is a fluid of zero viscosity, density ρ_s and velocity $\mathbf{v}_s$. The total density of helium II is $\rho = \rho_n + \rho_s$ and does not change significantly with temperature ($\rho \approx 0.145$ g/cm^3), whereas the relative proportions of ρ_n and ρ_s do, as shown in Fig. 1. At absolute zero $\rho_s/\rho = 1$ and $\rho_n/\rho = 0$, whereas at the lambda point $\rho_s/\rho = 0$ and $\rho_n/\rho = 1$. It is apparent from the figure that the normal fluid is effectively negligible for $T < 1$ K.

E-mail address: C.F.Barenghi@ncl.ac.uk (C.F. Barenghi).
URL: http://www.mas.ncl.ac.uk/~ncfb/ (C.F. Barenghi).

0997-7546/$ – see front matter
doi:10.1016/j.euromechflu.2003.10.011

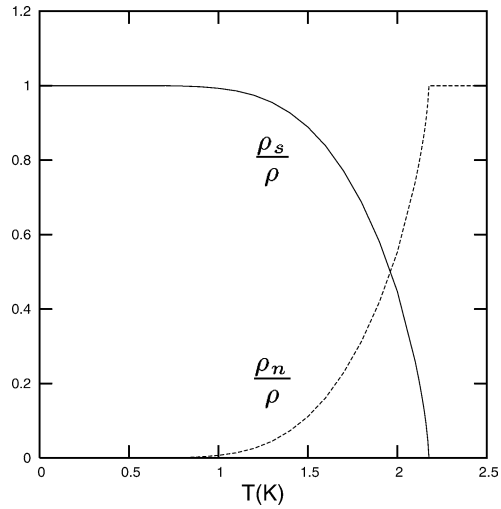

Fig. 1. Relative proportion of normal fluid and superfluid as a function of temperature.

Because of the presence of two separate fluid components, two-fluid hydrodynamics is different (at least at small velocities) from ordinary hydrodynamics. One example of non-classical behaviour is second sound, a wave motion in which temperature and entropy oscillate, $\mathbf{v}_n$ and $\mathbf{v}_s$ move in antiphase with respect to each other, and density and pressure remain essentially constant. In the context of helium II ordinary sound is called first sound, a wave in which density and pressure oscillate, entropy and temperature remain almost the same, and $\mathbf{v}_n$ and $\mathbf{v}_s$ move in phase with respect to each other. Second sound is important in turbulence because it is used to measure the amount of superfluid vorticity. A second example of non-classical behaviour is heat transfer. Consider a channel which is closed at one end and open to the helium bath at the other end. At the closed end a resistor dissipates a known heat flux W. With this set up and using an ordinary classical fluid (such as helium I), a temperature gradient can be measured along the channel, which indicates the existence of a finite thermal conductivity. If helium II is used, the heat is carried toward the bath by the normal fluid only, and $W = \rho S T v_n$ where S is the specific entropy. Because of the closed end of the channel, the mass flux is zero ($j = \rho_n v_n + \rho_s v_s = 0$), there is superfluid motion toward the heater ($v_s = -\rho_n v_n/\rho_s$), hence there is a net internal counterflow $v_n - v_s = W/(\rho_s S T)$ which is proportional to the applied heat flux W. This effect explains the remarkable ability of helium II to remove heat and makes helium II important in engineering applications.

3. The normal fluid

The normal fluid, at least in isolation, is very similar to a classical viscous fluid, so we expect that, when it is made turbulent, it consists of eddies of various sizes and strengths. It is therefore reasonable to expect that in the inertial range $1/\ell_0 < k < 1/\eta$ the energy spectrum $E(k)$ of the normal fluid is

$$E(k) = C\varepsilon^{2/3}k^{-5/3}, \tag{1}$$

where ε is the rate of energy dissipation per unit mass, C is a constant of order unity, ℓ_0 is the integral length scale (the scale at which energy is fed into the energy cascade), η is the Kolmogorov scale (the scale at which kinetic energy is dissipated by the action of viscosity), $E(k)$ is defined such that

$$\iiint \frac{1}{2}v_n^2 \,\mathrm{d}x\,\mathrm{d}y\,\mathrm{d}z = \int_0^\infty E(k)\,\mathrm{d}k, \tag{2}$$

and $k = |\mathbf{k}|$ is the magnitude of the three dimensional wavevector $\mathbf{k}$.

4. Superfluid vortex lines

The rotational motion of the superfluid is very different from the normal fluid's because it is constrained by quantum mechanics to discrete vortex filaments. The circulation around each superfluid vortex filament is fixed by the condition that

$$\oint_c \mathbf{v}_s \cdot \mathbf{dr} = \Gamma, \tag{3}$$

where c is any closed path around the axis of the vortex, $\Gamma = h/m \approx 9.97 \times 10^{-4}$ cm^2/sec is the quantum of circulation, h is Plank's constant and m is the mass of the helium atom. Using cylindrical coordinates (r, θ, z), assuming that the vortex is aligned in the z direction, Eq. (3) yields the classical azimuthal velocity field

$$v_{s\theta} = \frac{\Gamma}{2\pi r}. \tag{4}$$

Quantum mechanics also determines the superfluid vortex core structure, which is a hollow region of radius $a_0 \approx 10^{-8}$ cm only. There is no 'vortex stretching' of superfluid vortex lines in the usual sense of fluid mechanics: a superfluid vortex line can grow in length if energy is fed into it by the normal fluid, but the core radius must remain the same.

Superfluid turbulence therefore consists of a disordered, apparently random, tangle of very thin vortex filaments, as shown in Fig. 2. The figure is the result of a calculation performed using periodic boundary conditions: superfluid vortex lines, like classical vortex lines, are either closed loops or terminate at rigid walls.

Despite the lack of viscosity, superfluid vortex filaments can reconnect with each other, therefore the superfluid component of helium II is not exactly the same as a classical inviscid Euler fluid (whose vortices cannot reconnect). At temperatures above 1 K the normal fluid component starts having effects, and it must be noticed that the normal fluid and the superfluid vortex lines are coupled by a mutual friction force [2] which is proportional to the local velocity difference between the superfluid vortex line and the surrounding normal fluid.

Superfluid vortex lines appear at relatively low velocities, so the vortex tangle limits the otherwise perfect ability of helium II to transfer heat.

In the experiments the vortex tangle is detected by monitoring the attenuation of second sound, which is proportional to the vortex line density L (length of vortex line per unit volume). From the measurement of L, the average distance δ between vortices can be estimated as $\delta \approx L^{-1/2}$. The quantity $\omega_s = \Gamma L$ can be interpreted as the root mean square superfluid vorticity. The towed grid experiments performed by Donnelly and coworkers at the University of Oregon have produced values of ω_s over a six orders of magnitude range $10^{-2} < \omega_s < 10^4$ sec^{-1} [3].

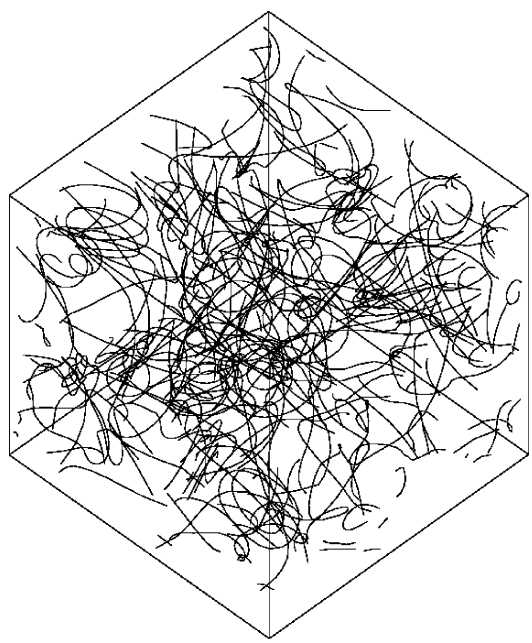

Fig. 2. Tangle of superfluid vortex filaments, calculation performed in a periodic box using the vortex filament model.

Finally, it must be noticed that the phenomenon of superfluidity (motion without friction) is limited not only by a critical temperature (as shown in Fig. 1) but also by a critical rotation (i.e., vorticity). A similar double limit in the form of a critical temperature and a critical magnetic field exists in the related phenomenon of superconductivity (motion without electrical resistance). In the case of superfluidity the second limit arises when the number of vortex lines is so large that the vortex core regions start overlapping. For helium II this limit is well beyond the experimental range (it can be estimated at $\omega_s \approx \Gamma/a_0^2 \approx 10^{13}$ sec^{-1}). However for the newly discovered superfluidity in atomic gases there is evidence [4] that this limit of extremely high density of vortex lines can be achieved in the laboratory.

5. Turbulence experiments

The turbulent flow of helium II has been the subject of many experiments. It is useful to distinguish between experiments performed at relatively high temperatures (in the region from $T = T_\lambda$ down to $T \approx 1$ K), and low temperature experiments ($T < 1$ K) for which the normal fluid (hence viscous dissipation) is effectively negligible.

In the high temperature range the surprising result is that turbulent helium II is very similar to ordinary (classical) turbulence. For example, it was found that if helium II is made turbulent by suddenly towing a grid in a sample initially at rest, the resulting turbulence decay obeys classical laws [5,6,3]. Classical results were also found by measuring mass flow rates and pressure drops along channels and pipes [7]. Furthermore, the classical drag crisis behind a sphere was observed [8]. Finally, when helium II was made turbulent by agitating it using counter-rotating propellers inside a closed cell, it was found that the energy spectrum obeys the classical Kolmogorov law [9] and is independent of T. These apparently classical results are at first surprising because helium II is a quantum fluid – it does not obey classical hydrodynamics but rather two-fluid hydrodynamics. It is also clear that the normal fluid alone cannot be held responsible for the apparent classical behaviour: Kolmogorov energy spectra were observed over the entire temperature range investigated, from $T = T_\lambda$ down to $T = 1.4$ K, a temperature so low that the normal fluid is not important ($\rho_n/\rho = 0.07$ only). Our aim is therefore to understand the experiments in terms of the basic fluid dynamics ingredients of the problem – the normal fluid, the superfluid vortex lines and their interaction.

The low temperature range refers to experiments performed using dilution refrigeration at temperatures as low as 20 mK [10]. In this regime, which is technically more difficult to study, superfluid turbulence is generated by a vibrating grid, and is observed to decay rapidly. The result raises the important question of what should be the fundamental mechanism to destroy kinetic energy in the absence of the normal fluid, hence without any known dissipative process, such as viscosity and friction.

6. Models of superfluid vortex lines

Two models of superfluid vortex line have been used to make progress into the problem. The first is the vortex filament model. Since the radius a_0 of the superfluid vortex core is many orders of magnitude smaller than the average separation δ between vortices or any other scale of interest in the flow, it is convenient to think of a superfluid vortex filament as a space curve $\mathbf{s} = \mathbf{s}(\xi, t)$ of infinitesimal thickness, where ξ is arc-length and t is time. It can be shown [11] that the curve moves with velocity approximately given by

$$\frac{\mathrm{d}\mathbf{s}}{\mathrm{d}t} = \mathbf{v}_{si} + \alpha \mathbf{s}' \times (\mathbf{v}_n - \mathbf{v}_{si}), \tag{5}$$

where α is a known temperature-dependent mutual friction coefficient [12], $\mathbf{v}_n$ is the prescribed normal fluid velocity, $\mathbf{s}' = \mathrm{d}\mathbf{s}/\mathrm{d}\xi$, and the self induced velocity $\mathbf{v}_{si}$ is given by the classical Biot–Savart integral

$$\mathbf{v}_{si}(\mathbf{s}) = \frac{\Gamma}{4\pi} \int \frac{(\mathbf{r} - \mathbf{s}) \times \mathbf{dr}}{|\mathbf{r} - \mathbf{s}|^3}. \tag{6}$$

In writing Eq. (5) a smaller transverse friction coefficient was neglected. To apply the model, an initial vortex configuration is discretized into a large number of points, which are then moved in time according to Eqs. (5) and (6). The equations must be supplemented with the extra assumption that two vortices reconnect when they come sufficiently close to each other. This assumption is justified by results obtained using the NLSE model, and the numerical technique to implement reconnections using vortex filaments is now standard [13]. The vortex tangle showed in Fig. 2 was produced using the vortex filament model.

A second model of a superfluid vortex line arises from the following nonlinear Schroedinger equation (NLSE) for the complex wave function ψ in the theory of a weakly interacting Bose–Einstein Condensate [14] (BEC):

$$\mathrm{i}\hbar \frac{\partial \psi}{\partial t} = -\frac{\hbar^2}{2m} \nabla^2 \psi + V_0 \psi |\psi|^2 - E_b \psi. \tag{7}$$

Here $\hbar = h/(2\pi)$, E_b is the chemical potential of a boson and V_0 is the strength of the repulsive interaction between bosons. Note that the number density $|\psi|^2$ has dimension of an inverse volume and that V_0 has dimension of an energy multiplied by a volume. By writing ψ in terms of the amplitude A and the phase ϕ, $\psi = A\exp(\mathrm{i}\phi)$, one finds from Eq. (7) the classical continuity equation

$$\frac{\partial \rho_s}{\partial t} + \nabla \cdot (\rho_s \mathbf{v}_s) = 0, \tag{8}$$

and the modified Euler equation

$$\rho_s \left(\frac{\partial v_{sj}}{\partial t} + v_{sk} \frac{\partial v_{sj}}{\partial x_k} \right) = -\frac{\partial P}{\partial x_j} + \frac{\partial \Sigma_{jk}}{\partial x_k}, \tag{9}$$

for the three components $j = 1, 2, 3$ of the superfluid velocity $\mathbf{v}_s$

$$\mathbf{v}_s = \frac{\hbar}{m} \nabla \phi. \tag{10}$$

In the NLSE model the superfluid density is

$$\rho_s = m A^2, \tag{11}$$

the pressure is

$$P = \frac{V_0 \rho_s^2}{2m^2}, \tag{12}$$

and the quantum stress is

$$\Sigma_{jk} = \frac{\hbar^2}{4m^2} \rho_s \frac{\partial^2 \ln(\rho_s)}{\partial x_j \partial x_k}. \tag{13}$$

Using cylindrical coordinates (r, θ, z) and setting the phase ϕ equal to the azimuthal angle θ, one recovers the velocity field (4) of a classical vortex line, and, by solving the remaining equation for ρ_s, one finds that $\rho_s \to 0$ as $r \to 0$ with the characteristic distance

$$a_0 = \frac{\hbar}{\sqrt{2mE_b}} \approx 10^{-8} \text{ cm}. \tag{14}$$

This quantity is the vortex core radius mentioned in the previous section.

It is important to notice that, since the superfluid density changes significantly only near the vortex cores, the quantum stress term is negligible in regions away from vortices, so in these regions the NLSE reduces to the Euler equation.

When two vortices approach each other at close distance, the quantum stress term becomes important and is responsible for the occurrence of vortex reconnections [15]. Note that the total energy is conserved in the NLSE model, so superfluid vortex reconnections, unlike reconnections in an ordinary fluid, do not require viscous dissipation of energy.

Finally, note that the NLSE model, unlike the vortex filament model, is compressible, therefore it allows sound generation. The main drawback of the NLSE model is that it refers to $T = 0$ only, so it is not possible to use it to understand finite temperature effects induced by the normal fluid.

7. Vortex reconnections

Numerical simulations of vortex tangles performed using the NLSE model revealed that, although the total energy is constant, the kinetic energy of the vortices decreases with time, whereas the level of sound energy increases [16]. The generation of sound is therefore the ultimate mechanism to destroy organised kinetic energy at absolute zero, in the absence of any other form of dissipation.

Recent work with the NLSE has highlighted the key role played by vortex reconnections in this process. For example, it was found that at the moment of reconnection, a sound wave in the form of an intense rarefaction pulse is generated [17] which removes kinetic energy from the vortex configuration. Fig. 3 shows the collision between two superfluid vortex rings calculated using the NLSE. The core regions are visualised by plotting isosurfaces of the density, and the sound pulse which results from the reconnection is the small dot at $t = 120$. The size of the pulse created by the reconnection is initially of the order of the core radius a_0, and its amplitude corresponds to a drop of ρ_s from the bulk value to zero. As the pulse moves away from the region of reconnection, its amplitude decreases and it spreads, as shown in Fig. 4.

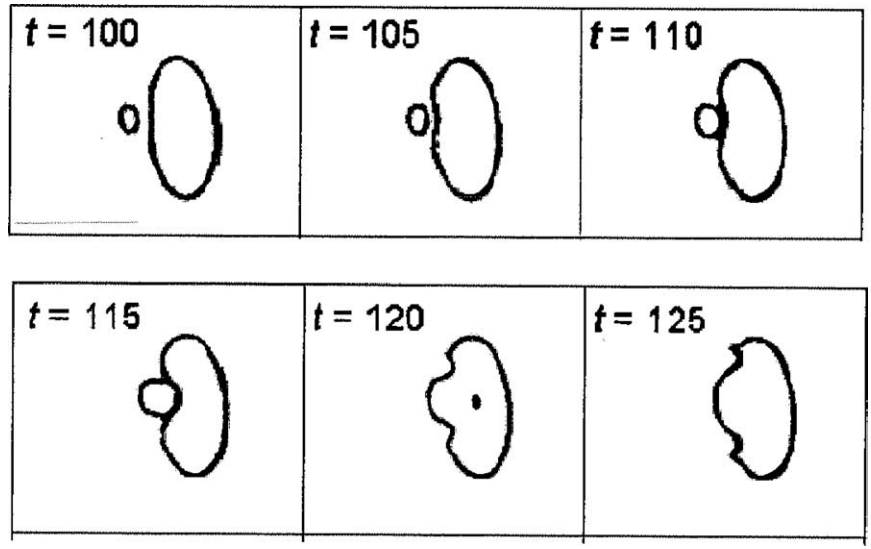

Fig. 3. Collision of two vortex rings [17]. Note the sound pulse in the middle of the vortex loop at $t = 120$ right after the reconnection event.

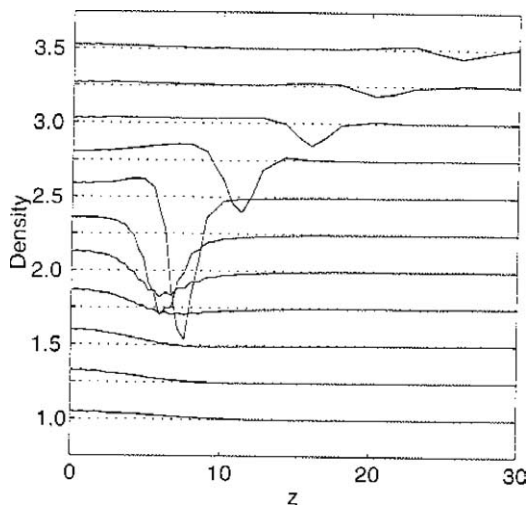

Fig. 4. Superfluid density profiles along the z axis for a collision of two vortex rings initially set on the x, y plane [17]. The curves correspond to profiles of the rarefaction sound pulse resulting from the reconnection at 11 different times and are offset by 0.25 from each other for clarity. The bulk density is normalised to unity for convenience.

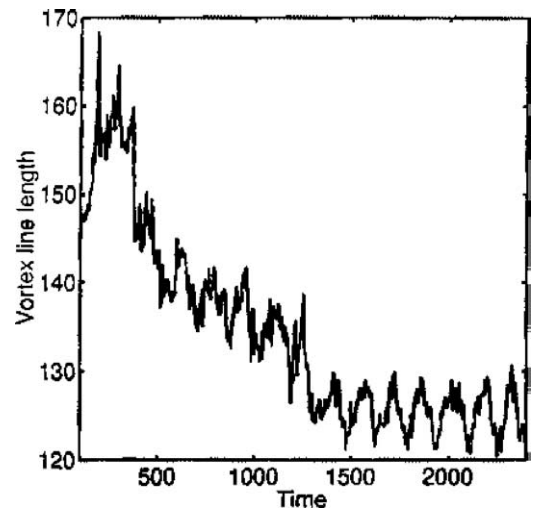

Fig. 5. Length of vortex line lost versus time calculated using the NLSE model [18].

It is well known from classical hydrodynamics that a rotating vortex produces sound. For example, if a straight vortex line is perturbed into a small amplitude helix of wavelength λ, the perturbation propagates as a Kelvin wave of one-dimensional Kelvin wavenumber k' (not to be confused with k) given by

$$k' = \frac{2\pi}{\lambda} \tag{15}$$

and angular velocity given by

$$\omega(k') = \frac{\Gamma}{4\pi} k'^2 \left[\log\left(\frac{2}{k' a_0} \right) - 0.5772 \right]. \tag{16}$$

Kelvin waves are continually excited within the vortex tangle by vortex reconnections; an example are the kinks visible in the last two frames of Fig. 3.

In the vortex tangle, emission of sound may take place in the form of isolated pulses as well as Kelvin wave radiation. Recently the NLSE was used to study the interaction of a system of four vortex rings which, after initial reconnections, evolved into a small tangle [18]. The kinetic energy of the vortices (measured in terms of length of vortex line) was computed during the evolution and the result is shown in Fig. 5. Loss of energy due to sound pulses and slower loss due to sound radiated by Kelvin waves is visible.

The power radiated by a Kelvin wave is negligible unless the angular frequency ω, hence the Kelvin wavenumber k', is very large [19,20]. For example, the power lost by dipolar radiation is proportional to k'^6. The question then arises of what process can excite Kelvin waves of sufficiently high wavenumber k' to radiate sound effectively and explain the decay of kinetic energy observed in the low temperature turbulence experiments.

The following numerical simulation performed using the vortex filament method at $T = 0$ shed some light into the problem [21]. The calculation started with four vortex rings placed symmetrically around a cube and launched against each other (see Fig. 6(a)). Shortly after the rings' reconnections (Fig. 6(b)) the cusps left on the vortex filaments by the reconnection events evolved into large amplitude Kelvin waves (Fig. 6(c)) which interacted and generated Kelvin waves of higher and higher Kelvin wavenumbers (Fig. 6(d)). Note the crinkled appearance of the vortices – in this calculation there is no friction to damp high wavenumber waves and smooth the vortices (effective damping occurs only at high k' due to the finite numerical discretization). The authors found that the energy spectrum of this Kelvin wave cascade obeys a k^{-1} power law; they also argued that the Kelvin wave cascade is responsible for the generation of the high wavenumbers required to radiate sound efficiently.

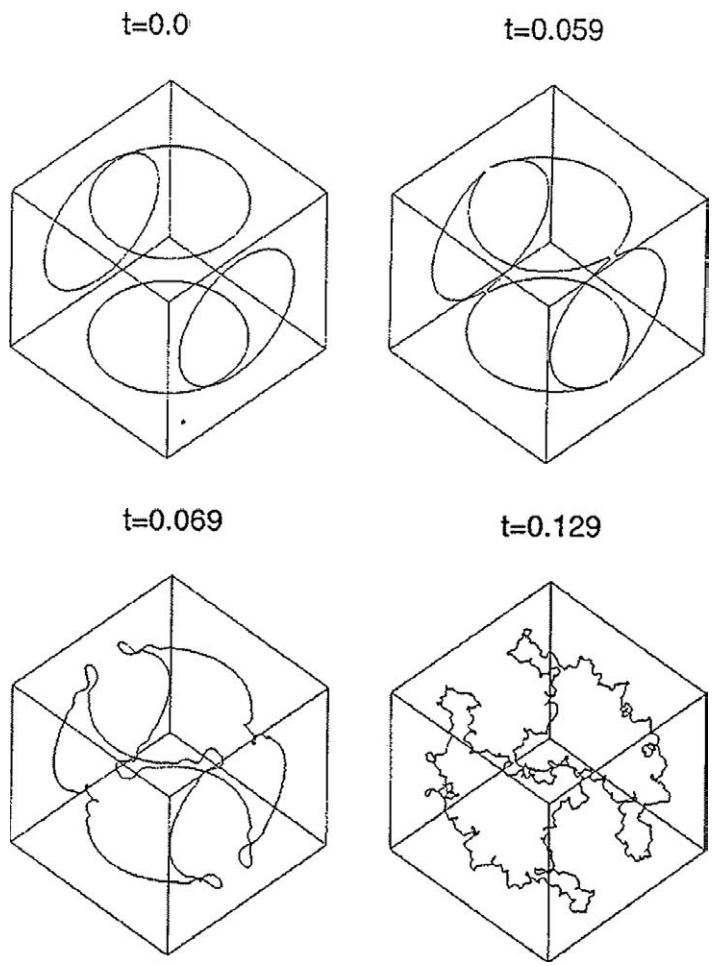

Fig. 6. Collision of four vortex rings and generation of Kelvin waves of high wavenumber [21].

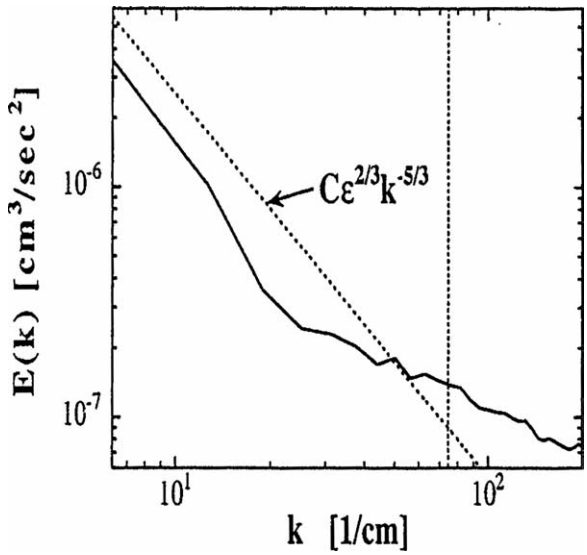

Fig. 7. Energy spectrum of a superfluid vortex tangle at absolute zero calculated using the vortex filament model [22].

8. Energy spectrum of superfluid turbulence at absolute zero

The results described above indicate that, in the absence of normal fluid ($T = 0$), the generation of sound is the plausible sink of kinetic energy. The effect suggests that Kolmogorov's theory can be applied. If energy is fed into the vortex system at large scales ℓ_0, if there is an inertial range of wavenumbers and if a sink of energy exists at high wavenumbers, then the superfluid energy spectrum should scale as $E(k) \sim k^{-5/3}$, like the normal fluid's spectrum.

Evidence that Kolmogorov's $k^{-5/3}$ law applies to superfluid turbulence at $T = 0$ was first discovered using the NLSE model [16]. The authors also noticed that at wavenumbers larger than $1/\delta$ the spectrum assumed a k^{-1} dependence which they attributed to the contribution of individual vortex lines (from results obtained recently, it is more likely that the k^{-1} dependence arises from the Kelvin wave cascade). Unfortunately the calculation lacked convincing numerical resolution at low k. The problem is that when using the NLSE model one must numerically resolve the changing shape of ψ in the core of each vortex filament, which limits the number of vortices of the computation.

More recently a similar calculation was attempted using the vortex filament model at $T = 0$ [22]. The authors confirmed the $k^{-5/3}$ law, as shown in Fig. 7. The vertical dashed line in the figure corresponds to the wavenumber $k_\delta = 1/\delta$. The result is consistent with the scenario that $E \sim k^{-5/3}$ for $k < k_\delta$ and $E \sim k^{-1}$ for $k > k_\delta$ which we describe [20]. Note that in this calculation the energy sink was not the generation of sound, which is absent in the vortex filament model, but rather the finite discretization along the filaments which removes Kelvin waves of high wavenumbers. The result is important because it confirms the previous finding with a different model, but unfortunately the numerical resolution of the spectrum at $k \ll k_\delta$ is still relatively poor (what limits the calculation in this case is the computational cost of the Biot–Savart law to achieve the intense vortex tangle necessary to explore the region $k \ll k_\delta$).

9. Energy spectrum of superfluid turbulence at finite temperature

We have found that both the normal fluid and the superfluid should have independent reasons to obey Kolmogorov's $k^{-5/3}$ law. The energy sink of the normal fluid is viscous dissipation, whereas that of the superfluid should be sound generation. The natural question to ask is what is the energy spectrum of helium II at temperatures above 1 K, in the presence of the normal fluid, and what is the role played by the mutual friction.

It has been argued [19,20] that at spatial scales larger than the average distance δ between vortices the normal fluid and the superfluid vortices are coupled by a small degree of polarization of the almost random tangle of superfluid vortex lines. If that is the case, on these scales helium II behaves as a single fluid of density $\rho = \rho_n + \rho_s$. This is consistent with the experiments, for example with the observation that the energy spectrum is independent of temperatures and obeys Kolmogorov's law [9].

Simple theoretical models of polarization have been recently suggested [23]. For example, the authors considered a straight superfluid vortex segment which points away from the origin in the presence of a given normal fluid rotation. Using spherical

coordinates (r, θ, ϕ), they assumed that the vortex is initially in the plane $\theta = \pi/2$ and that the normal fluid's velocity is $\mathbf{v}_n = (0, 0, \Omega r \sin\theta)$. The motion of the vortex segment is determined by Eq. (5), for which one has

$$\frac{\mathrm{d}\theta}{\mathrm{d}t} = -\alpha\Omega \sin(\theta), \tag{17}$$

together with $\mathrm{d}r/\mathrm{d}t = 0$ and $\mathrm{d}\phi/\mathrm{d}t = 0$. The solution is

$$\theta(t) = 2\tan^{-1}\left(\mathrm{e}^{-\alpha\Omega t}\right), \tag{18}$$

with r and ϕ constant. Given enough time, the vortex segment will align along the direction of the normal fluid rotation ($\theta \to 0$ for $t \to \infty$). However, if $\mathbf{v}_n$ represents a turbulent eddy, its lifetime is only of the order of $\tau \approx 1/\Omega$, and since the temperature dependent mutual friction coefficient α is less or much less than unity, the superfluid vortex can only turn to the angle $\theta(\tau) \approx \pi/2 - \alpha$. Despite the smallness of the angle, this effect is sufficient to create a net polarization of the tangle in the direction of the normal fluid's rotation, provided that there are enough vortices. To see this, assume that the energy spectrum $E(k)$ of the normal fluid is given by Kolmogorov's expression Eq. (1). In the time $1/\omega(k)$, where $\omega(k) = \sqrt{k^3 E(k)}$, re-ordering of existing vortex lines creates a net superfluid vorticity $\omega_s \approx \alpha L \Gamma/3$ in the direction of the vorticity $\omega(k)$ of the driving normal fluid eddy of wavenumber k. Matching ω_s and $\omega(k)$ would then require

$$\frac{1}{3}\alpha\Gamma L \geqslant C^{1/2}\varepsilon^{1/3}k^{2/3}. \tag{19}$$

The normal fluid vorticity increases with k and is concentrated at the smallest scale ($k \approx 1/\eta$), so a vortex tangle with a given value of L may satisfy the above equation only up to a certain critical wavenumber k_c. Substituting $\varepsilon = \nu_n^3/\eta^4$ where ν_n is the normal fluid's kinematic viscosity (the viscosity of helium II divided by ρ_n), we obtain $\delta/\eta = C^{-1/4}(\alpha/3)^{1/2}(\Gamma/\nu_n)^{1/2}(\eta k_c)^{-1/3}$. Setting $k_c \approx 1/\eta$ one has then

$$\frac{\delta}{\eta} = C^{-1/4}\left(\frac{\alpha}{3}\right)^{1/2}\left(\frac{\Gamma}{\nu_n}\right)^{1/2}. \tag{20}$$

In the temperature range of experimental interest Γ/ν_n ranges from 0.43 at $T = 1.3$ K to 5.86 at $T = 2.15$ K, so $\delta/\eta = \mathrm{O}(1)$ and one concludes that matching of normal fluid and superfluid vorticities ($k_c \approx 1/\eta$) is possible throughout the inertial range.

Numerical evidence of polarization at finite T was found recently using the vortex filament model [23]. The authors studied the reaction of an initially random tangle of superfluid vortex filaments to a normal fluid ABC flow [24] given by

$$v_{nx} = A\sin(kz) + C\cos(ky), \tag{21}$$

$$v_{ny} = B\sin(kx) + A\cos(kz), \tag{22}$$

$$v_{nz} = C\sin(ky) + B\cos(kx), \tag{23}$$

where k is the wavenumber and the parameters are set to $A = B = C$ for simplicity. The advantage of the ABC flow is that it is relatively complex but has a single scale, so it is possible to calculate enough superfluid vortices within that scale. Calculations were performed choosing values of α and A corresponding to a variety of temperatures and normal fluid velocities. The initial conditions consisted of superfluid vortex rings at random positions and with random orientations. During the evolution the quantity $\langle\cos(\theta)\rangle$ was monitored, which is the tangle – averaged projection of the local tangent to a vortex in the direction of the local normal fluid vorticity:

$$\left\langle\cos(\theta)\right\rangle = \langle \mathbf{s}' \cdot \widehat{\boldsymbol{\omega}}_n \rangle, \tag{24}$$

where $\widehat{\boldsymbol{\omega}}_n = (1/\omega_n)\boldsymbol{\omega}_n$ and $\boldsymbol{\omega}_n = \nabla \times \mathbf{v}_n$. At $t = 0 \langle\cos(\theta)\rangle = 0$ due to the random nature of the initial state. It was found that the superfluid vortex length increased or decreased depending on whether the ABC flow was strong enough to feed energy into the normal fluid via instabilities of vortex waves, but in all cases $\langle\cos(\theta)\rangle$ increased with time. From the simple model described above one expects that the polarization induced by the normal fluid vorticity is proportional to α. This is confirmed by the result of the calculation presented in Fig. 8: no matter whether the tangle grows or decays, approximately the same relative polarization $P = \langle\cos(\theta)\rangle/\alpha$ takes place within the relative lifetime of the normal fluid eddy $t' = t/\tau < 1$, where $\tau = 1/\omega_n$ with $\omega_n = \sqrt{3}Ak$.

Polarization driven by friction with the normal fluid is also important in rotating superfluid turbulence, which is currently a topic of great theoretical [25] and experimental interest [26]. The polarization of vortex lines described here is analogous to the tendency of small scale vortex tubes in classical turbulence to align with the direction of rotation in rotating turbulence [27].

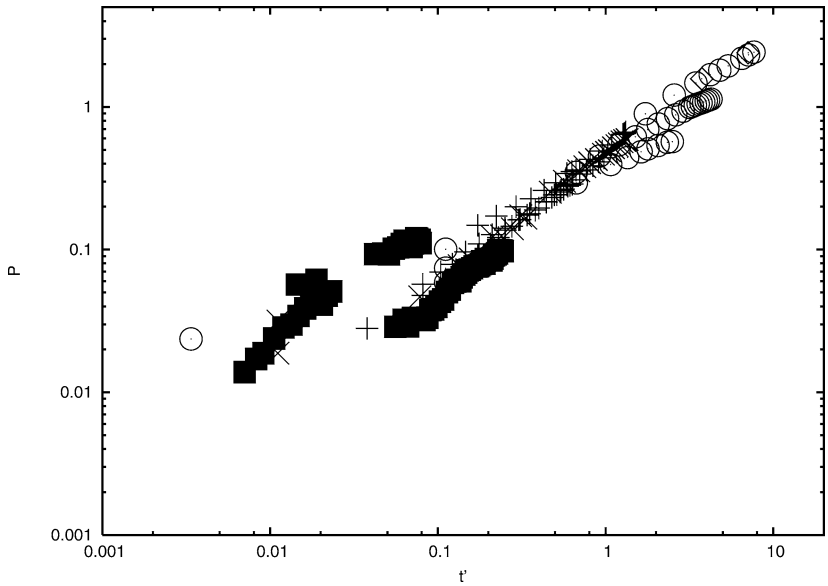

Fig. 8. Polarization of superfluid turbulence [23]. The figure shows $P = \langle \cos(\theta) \rangle / \alpha$ versus scaled time $t' = t/\tau$ where τ is the eddy's lifetime. The symbols correspond to a variety of temperatures and normal fluid velocities.

10. Discussion

This review of the most recent results indicates that the observation of turbulence decay at temperatures so low that viscous dissipation can be neglected can be explained, at least in principle, by the transformation of kinetic energy into sound energy. Furthermore, if sound is an energy sink for the superfluid (in analogy to viscosity as the energy sink for the normal fluid), then it is plausible that the energy spectrum of a superfluid tangle obeys the classical Kolmogorov's $k^{-5/3}$ law. Finally, the mutual friction seems to be able to polarise the vortex tangle by a sufficient amount to explain the coupling between normal fluid and superfluid vorticities at all wavenumbers of the inertial range. Taken together, these results indicate great similarity between turbulence in helium II and classical turbulence as far as velocity fields and energy spectra are concerned, and are consistent with the observations.

However the scenario described above is still incomplete and qualitative and still needs firm confirmation. For example, the acoustic sink of energy at high wavenumbers may not be uncorrelated with smaller wavenumbers via the spatial nonlocality of acoustic waves, thus preventing the existence of an inertial range as in classical fluid dynamics. Better numerical evidence for the $k^{-5/3}$ dependence of the superfluid energy spectrum in the region $k < k_\delta$ is clearly needed, either using the NLSE model or the vortex filament model. Above all, theoretical understanding of the Kelvin energy cascade is needed in order to make comparison with experiments. Another problem is that rarefaction pulses following an individual vortex reconnection are a consequence of the NLSE but have not been observed directly in the laboratory, which is not surprisingly given the extremely small length and time scales involved. It is possible that the NLSE, which is currently proving a very good model of superfluidity in atomic condensates, fails to model helium II in this respect (helium II is not a weakly interacting gas but a liquid). Fortunately the field of atomic BEC is progressing very rapidly and in the near future it should be possible to study with better resolution the same problem of turbulence near absolute zero which is currently being studied in helium II. If rarefaction pulses exist as predicted, the relative importance of Kelvin wave radiation and emission of sound pulses must be analysed, as it may depend on the vortex line density. Finally, the nonlinear saturation of the polarization process must be understood.

A major step forward would be to overcome the major limitation of the vortex filament method as currently used in the study of turbulence, that the normal fluid velocity is prescribed rather than computed. Until now the back reaction of the superfluid vortices onto $\mathbf{v}_n$ has been studied only for the very simple geometry of a single superfluid vortex ring [28], but in general one should determine the evolution of $\mathbf{v}_n$ by solving the Navier–Stokes equation modified by the introduction of a mutual friction term.

Surprisingly, the main difference between quantum turbulence and classical turbulence may turn out to be the spectrum of the pressure. It has been recently predicted in fact that, due to the extreme localisation in space of the superfluid vorticity, pressure spectra in helium II should follow a k^{-2} scaling in contrast with the classical $k^{-7/3}$ pressure scaling of Kolmogorov's theory [29]. This result, if confirmed experimentally, would represent a striking macroscopic consequence of quantum theory.

On the experimental side, it is important to obtain better energy spectra using smaller probes, and to develop techniques to learn more about the motion of the normal fluid. In classical fluid dynamics it is usually relatively easy to visualise the velocity field but relatively difficult to have information about the vorticity. Paradoxically, existing flow visualisation near absolute zero gives much information about the vorticity of the superfluid (via the second sound technique), but we know very little of the classical-like normal fluid.

Acknowledgements

I am grateful to W.F. Vinen and M. Tsubota for useful discussions.

References

[1] R.J. Donnelly, Quantized Vortices in Helium II, Cambridge University Press, 1991.
[2] C.F. Barenghi, R.J. Donnelly, W.F. Vinen, Friction on quantized vortices in helium II. A review, J. Low Temp. Phys. 52 (1983) 189.
[3] L. Skrbek, J.J. Niemela, R.J. Donnelly, Four regimes of decaying grid turbulence in a finite channel, Rev. Lett. 85 (2000) 2973.
[4] F. Chevy, K.W. Madison, J. Dalibard, Measurement of the angular momentum of a rotating Bose–Einstein condensate, Phys. Rev. Lett. 85 (2000) 2223.
[5] M.R. Smith, R.J. Donnelly, N. Goldenfeld, W.F. Vinen, Decay of vorticity in homogeneous turbulence, Phys. Rev. Lett. 71 (1993) 2583.
[6] S.R. Stalp, L. Skrbek, R.J. Donnelly, Decay of grid turbulence in a finite channel, Phys. Rev. Lett. 82 (1999) 4831.
[7] P.L. Walstrom, J.G. Weisend, J.R. Maddocks, S.W. VanSciver, Turbulent-flow pressure-drop in various HeII transfer system components, Cryogenics 28 (1998) 101.
[8] M.R. Smith, D.K. Hilton, S.V. VanSciver, Observed drag crisis on a sphere in flowing HeI and HeII, Phys. Fluids 11 (1999) 751.
[9] J. Maurer, P. Tabeling, Local investigation of superfluid turbulence, Europhys. Lett. 43 (1998) 29.
[10] S.I. Davis, P.C. Hendry, P.V.E. McClintock, Decay of quantized vorticity in superfluid He-4 at mK temperatures, Physica B 280 (2000) 43.
[11] K.W. Schwarz, Three-dimensional vortex dynamics in superfluid He-4. Homogeneous superfluid turbulence, Phys. Rev. B 38 (1988) 2398.
[12] R.J. Donnelly, C.F. Barenghi, The observed properties of liquid helium at the saturated vapor pressure, J. Phys. Chem. Reference Data 27 (1998) 1217.
[13] D.C. Samuels, Vortex filaments methods for superfluids, in: C.F. Barenghi, R.J. Donnelly, W.F. Vinen (Eds.), Quantized Vortex Dynamics and Superfluid Turbulence, Springer, Heidelberg, 2001.
[14] P.H. Roberts, N.G. Berloff, The nonlinear Schrödinger equation as a model of superfluidity, in: C.F. Barenghi, R.J. Donnelly, W.F. Vinen (Eds.), Quantized Vortex Dynamics and Superfluid Turbulence, Springer, Heidelberg, 2001.
[15] J. Koplik, H. Levine, Vortex reconnection in superfluid helium, Phys. Rev. Lett. 71 (1993) 1375–1378.
[16] C. Nore, M. Abid, M.E. Brachet, Kolmogorov turbulence in low temperatures superflows, Phys. Rev. Lett. 78 (1997) 3896.
[17] M. Leadbeater, T. Winiecki, D.C. Samuels, C.F. Barenghi, C.S. Adams, Sound emission due to superfluid vortex reconnections, Phys. Rev. Lett. 86 (2001) 1410.
[18] M. Leadbeater, D.C. Samuels, C.F. Barenghi, C.S. Adams, Decay of superfluid turbulence via Kelvin-wave radiation, Phys. Rev. A 67 (2003) 015601.
[19] F. Vinen, Classical character of turbulence in a quantum liquid, Phys. Rev. B 61 (2000) 1410;
F. Vinen, Decay of superfluid turbulence at very low temperature: the radiation of sound from a Kelvin wave on a quantized vortex, Phys. Rev. B 64 (13) (2001) 134520.
[20] W.F. Vinen, J.J. Niemela, Quantum turbulence, J. Low Temp. Phys. 129 (2002) 213.
[21] D. Kivotides, J.C. Vassilicos, D.C. Samuels, C.F. Barenghi, Kelvin waves cascades in superfluid turbulence, Phys. Rev. Lett. 86 (2001) 3080.
[22] T. Araki, M. Tsubota, S.K. Nemirovskii, Energy spectrum of superfluid turbulence with no normal fluid component, Phys. Rev. Lett. 89 (2002) 145301.
[23] C.F. Barenghi, S. Hulton, D.C. Samuels, Polarization of superfluid turbulence, Phys. Rev. Lett. 89 (2002) 275301.
[24] T. Dombre, U. Frisch, J.M. Greene, M. Henon, A. Mehr, A.M. Soward, Chaotic streamlines in the ABC flows, J. Fluid Mech. 167 (1986) 353.
[25] M. Tsubota, T. Araki, C.F. Barenghi, Rotating superfluid turbulence, Phys. Rev. Lett. 90 (2003) 205301.
[26] A.P. Finne, T. Araki, R. Blaauwgeers, V.B. Eltsov, N.B. Kopnin, M. Krusius, L. Skrbek, M. Tsubota, G.E. Volovik, An intrinsic velocity-independent criterion for superfluid turbulence, Nature 424 (2003) 1022.
[27] C. Cambon, J.F. Scott, Linear and nonlinear models of anisotropic turbulence, Annu. Rev. Fluid Mech. 31 (1999) 1.
[28] D. Kivotides, C.F. Barenghi, D.C. Samuels, Triple vortex ring structure in superfluid helium II, Science 290 (2000) 777.
[29] D. Kivotides, J.C. Vassilicos, C.F. Barenghi, M.A.I. Khan, D.C. Samuels, Quantum signature of superfluid turbulence, Phys. Rev. Lett. 87 (2001) 275302.